analytical chemistry

ARTICLE

pubs.acs.org/ac

# General Approach for Monitoring Peptide−Protein Interactions Based on Graphene−Peptide Complex

Chun-Hua Lu, Juan Li, Xiao-Long Zhang, Ai-Xian Zheng, Huang-Hao Yang,* Xi Chen, and Guo-Nan Chen

The Key Lab of Analysis and Detection Technology for Food Safety of the Ministry of Education, Fujian Provincial Key Laboratory of Analysis, Detection Technology for Food Safety, College of Chemistry, Chemical Engineering, Fuzhou University, Fuzhou 350002, People's Republic of China

Supporting Information

**ABSTRACT:** Peptide−protein interactions have critical roles in biology. Monitoring peptide−protein interactions plays an important role in investigating molecular recognition, screening drugs, and designing biosensors. In this paper, we develop a novel fluorescent approach to monitor peptide−protein interactions based on the assembly of pyrene-labeled peptide and graphene oxide (GO). The pyrene-labeled peptide is strongly adsorbed on the surface of GO via $\pi-\pi$ interactions and hydrophobic interactions. As a result, the proximity of the GO to the pyrene moiety effectively quenches the fluorescence of pyrene. In the presence of target protein, the competitive binding of the target protein with GO for peptide results in the restoration of fluorescence signal. This signaling mechanism makes it possible to monitor the peptide−protein interactions in a homogeneous real-time format.

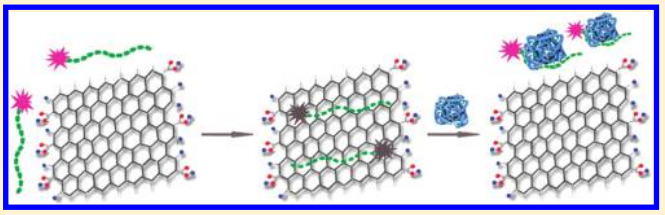

Protein−protein and peptide−protein interactions have critical roles in biology.[1,2] Both chemical and biological approaches to detect and study peptide−protein interaction will provide a deeper understanding of the nature, regulation, and function of these interactions, which is central to human health.[3,4] Furthermore, with the development of phage display and other in vitro selection techniques, an increasing number of peptides with specific binding affinity to a wide range of macromolecular targets are being produced.[5,6] Such peptides can serve as potential recognition elements for sensors. Therefore, studying the interactions between peptides and target molecules has attracted considerable attention in investigating molecular recognition, screening drugs, and designing biosensors.[7,8]

However, the design of peptide-based sensors that report on the interactions with specific targets is challenging, owing to the lack of easily measurable output signal. Up to now, enormous effort has gone into the development of viable biosensors to study peptide−protein interactions.[9−12] Fluorescence spectroscopy is a powerful tool for monitoring biological events due to its rapidness, simplicity, sensitivity, and reproducibility. Recently, many peptide-based optical sensing approaches using fluorescence resonance energy transfer (FRET) between the fluorophores and quenchers modified at terminal ends of peptides to study peptide−protein interactions have been developed.[13−18] However, these approaches require the peptide to undergo a conformational change in response to the binding of protein. Such a conformational change leads to distance changes between the fluorophores and quenchers, resulting in the measurable signal output. Inspired by DNA molecular beacons, a new platform named peptide beacons (PBs) has been developed, and initial attempts to utilize them for detecting targets have yielded rather promising results.[19−21] However, they are hard to design in a way that they form stable stem−loop structures. To surmount this, Plaxco's group and Seitz's group developed a new and ingenious kind of PBs containing a peptide recognition element flanked by peptide nucleic acid (PNA) sequences that hybridize to form a double-stranded stem, which was more closely analogous to DNA molecular beacons.[22,23] Although they were shown to be general, sensitive, and specific, they require expensive modification of PNA and the fluorophore/quencher pair. Therefore, there is still a great demand for developing simple, general, and effective approaches to monitor peptide−targets interactions at low cost.

Herein, we develop a simple and general approach for monitoring peptide−protein interactions based on graphene and pyrene-labeled peptide complex (Scheme 1). Graphene, graphene oxide (GO), and their derivatives are emerging materials capable of remarkable electronic, mechanical, and thermal properties.[24−26] Recently, they have been shown to enable fascinating applications in biological field, including biosensors[27−32] and drug delivery.[33−35] Pyrene-based fluorophores exhibit large extinction coefficients, excellent quantum yields, and good stability in aqueous solution.[36] On the basis of these attributes, pyrene has been employed as an optical reporter in molecular beacons[19,37] and for detection of infectious prion proteins.[38] In addition, pyrene and its derivatives are well-known for their noncovalent interactions with molecules having $\pi$-electron-rich frameworks, such as carbon nanotubes and graphene.[39−42]

**Received:** March 9, 2011
**Accepted:** August 22, 2011
**Published:** August 22, 2011

**Scheme 1. Schematic Illustration of the Concept of Using Pyrene-Labeled Peptide and GO To Monitor Protein−Peptide Interactions**

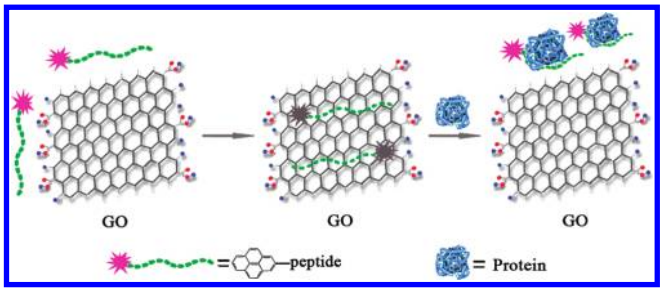


**Table 1. Sequences of the Used Peptides (from N-Terminus to C-Terminus)**

| type | sequence |
|---|---|
| P1 | pyrene−GGGRKRIHIGPGPAFYTT |
| P2 | pyrene−GGGNSWGCAFRQVC |

Therefore, in our approach, pyrene acts not only as a signal reporter but also as an "adhesion agent" to enhance the interaction between peptide and GO. The pyrene-labeled peptide could strongly adsorb on the surface of GO via $\pi-\pi$ interactions and hydrophobic interactions. As a result, the proximity of the GO to pyrene moiety effectively quenches the fluorescence of pyrene through energy-transfer or electron-transfer processes.[39−42] However, in the presence of target protein, the competitive binding of the target protein with GO for pyrene-labeled peptide results in desorption of pyrene-labeled peptide from the surface of GO. In turn, the initially quenched fluorescence of pyrene is recovered.

## EXPERIMENTAL SECTION

**Materials.** Graphite power of analytical grade was from Sinopharm Chemical Reagent Co. Ltd. (China). Both peptides were synthesized by GL Biochem (Shanghai) Ltd. The peptides were labeled with 1-pyrenebutyric acid at their N-terminus, which were purified by HPLC and confirmed by mass spectrometry. Ultrapure water obtained from a Millipore water purification system (18 MΩ cm resistivity) was used in all runs. All other reagents were of analytical grade. Table 1 shows the sequences of the used peptides.

**Synthesis of Graphene Oxide.** Graphene oxide (GO) was synthesized from natural graphite powder by a modified Hummer's method.[43] Briefly, graphite powder (2 g) was ground with NaCl to reduce the particle size. After removing the salt, the graphite was added to the concentrated $H_2SO_4$ (80 mL) and left stirring for 2 h. Afterward, $KMnO_4$ (10 g) was added gradually under stirring and the temperature of the mixture was kept to less than 20 °C. Successively, the mixture was stirred at 35 °C for 2 h. Keeping the temperature less than 50 °C, distilled water (180 mL) was added, and then the mixture was stirred at room temperature for 3 h. The reaction was ended by a final addition of distilled water (450 mL) and $H_2O_2$ (30% v/v aqueous solution, 20 mL). At the end, the mixture was repeated washed with diluted HCl (3.7 wt %) aqueous solution and then distilled water. Exfoliation was carried out by sonicating graphene oxide (2 mg/mL) dispersion under ambient condition for 4 h. Finally, the product was further purified by dialysis for 1 week to remove the remaining metal species.

**Monitoring the Interactions between Peptide and Protein.** Standard protein solutions were prepared by serial dilution starting with 0.05 mol/L phosphate buffer (PBS, pH 7.4). Pyrene-labeled peptides (P1 or P2) were resuspended by first dissolving in dimethyl sulfoxide (DMSO) (about 3% of the final volume) and then further diluting with buffer to obtain the desired concentration. P1 or P2 (2 $\mu$M) were mixed with GO for 5 min prior to the addition of protein. The final protein concentration in samples ranged from 0 to 50 nM. After allowing this mixture to stand for about 30 min at room temperature, the fluorescence of the mixture was detected.

Human serum samples were supported by the hospital of the Fuzhou University. The samples were centrifuged about 10 min at 1000 rpm. Then, the supernatants were collected and diluted to 20% by buffer (0.05 mol/L PBS, pH 7.4). The saliva samples were obtained from laboratory personnel.

**Apparatus and Methods.** Atomic force microscopic (AFM) images were taken out using a Nanoscope III a multimode atomic force microscope (Veeco Instruments, U.S.A.) in tapping mode to simultaneously collect height and phase data. Raman spectra were recorded at ambient temperature on a Renishaw InVia Raman spectrometer with an excitation laser at 785 nm. The Fourier transform infrared spectroscopy (FT-IR) spectrum was recorded on a Nicolet 6700 spectrometer (Thermo Electron Corporation). X-ray diffraction (XRD) patterns were obtained by using an X-ray power diffraction meter (D/MAX-3C, Rigaku Co., Japan). Fluorescence spectra, intensity, and anisotropy measurements were taken with a FLS 920 fluorescence spectrometer (Edinburgh Instruments Ltd., U.K.). The temperature was maintained at 25 °C. The reported anisotropy values are an average of four independent measurements.

## RESULTS AND DISCUSSION

**Characterization of GO.** Figure 1A shows XRD patterns of GO and graphite. The pattern of GO reveals a sharp 002 reflection at $2\theta$ = 10.3°. The most intense peak for graphite is at $2\theta$ = 26.4°. After oxidation, the interlay space of GO is larger than that of the graphite, as a result of the introduction of oxygenated functional groups on carbon sheets. Figure 1B shows the AFM image of GO in tapping mode to simultaneously collect height and phase data. The sample used for AFM observation was prepared by depositing a droplet of GO dispersion on a freshly cleaved mica surface and drying it under vacuum at room temperature. The average thickness of the GO sheet was about 1 nm, which matches well with the reported apparent thickness of GO.[27]

The FT-IR and Raman spectra of GO further provided the information of the successful synthesis of GO. As shown in Figure 2A, the FT-IR spectrum gives the characteristic vibrations of GO and graphite and matches well with that reported previously.[32] The characteristic vibrations of GO are a broad and intense peak of O−H group at 3400 $cm^{-1}$, a C═O peak at 1730 $cm^{-1}$, a C−OH stretching peak at 1220 $cm^{-1}$, an C−O stretching peak at 1050 $cm^{-1}$, and a peak attributed to the vibrations of unoxidized graphitic skeletal domains and the adsorbed water molecules at 1620 $cm^{-1}$. As for graphite, the spectrum is essentially featureless except the C═C conjugation at 1590 $cm^{-1}$ and O−H group at 3409 $cm^{-1}$. Figure 2B shows the Raman spectrum of GO and graphite. The Raman spectrum

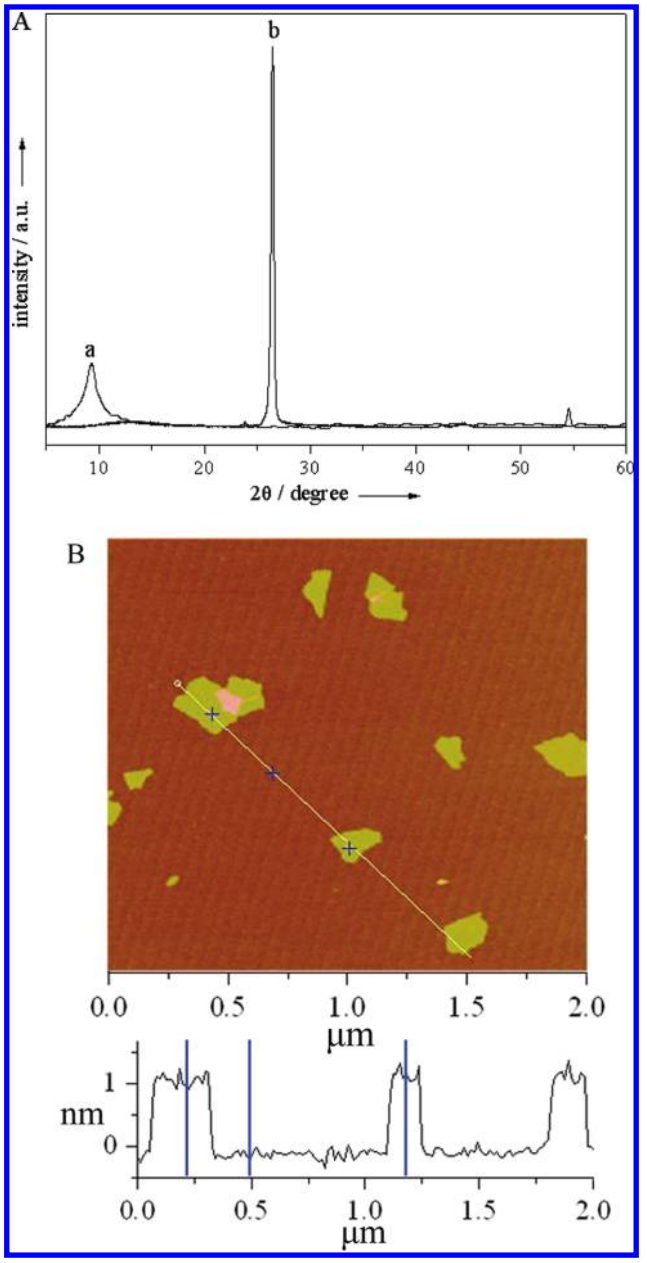


**Figure 1.** (A) XRD patterns of GO (a) and graphite (b). (B) AFM height image of GO deposited on mica substrates.

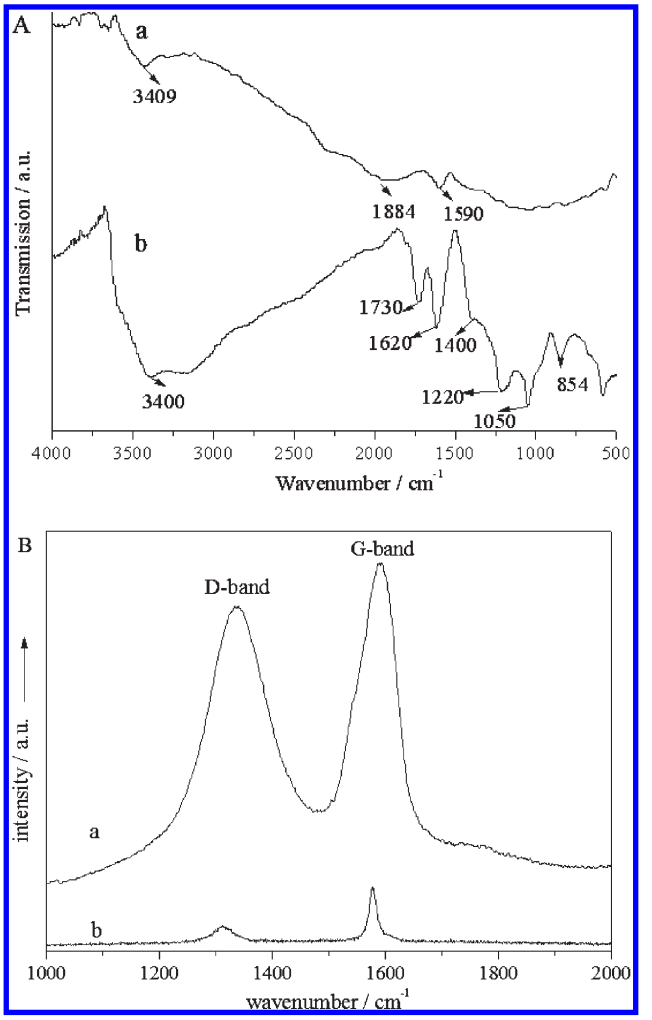


**Figure 2.** (A) FT-IR spectra of (a) graphite and (b) GO. The absorption peak wavelengths are indicated. (B) Raman spectra of (a) GO and (b) graphite.

of graphite showed a strong peak assigned to the vibration of $sp^2$-bonded carbon atoms at 1597 $cm^{-1}$ (G band) and a very weak peak assigned to the vibration of carbon atoms with dangling bonds in plane terminations of disordered graphite at 1337 $cm^{-1}$ (D band). However, the Raman spectrum of GO showed the well-documented D and G bands. This phenomenon agreed well with that reported previously and indicated the formation of some $sp^3$ carbon in GO.[44]

**Monitoring the Interactions between Peptide and Anti-HIV-1 gp120 Antibody.** To demonstrate the utility of our approach, we synthesized a pyrene-labeled peptide directed against an antibody diagnostic of HIV infection. The human immunodeficiency virus type 1 (HIV-1) glycoprotein gp120 is an important protein with a role in receptor binding and membrane fusion.[45,46] We employed a highly antigenic, V3-region peptide (P1) present in the gp120 protein[47] for detection of anti-HIV-1 gp120 antibody (Ab1). We first studied the interaction of P1 with GO. Once P1 was adsorbed on the basal planes of GO, it underwent strong $\pi-\pi$ interactions with GO via its pyrene moiety. Hydrophobic interactions and $\pi-\pi$ interactions between the flat planar graphene sheets and the aromatic rings of the amino acids in P1 may also facilitate P1 binding to GO.[48] The P1−GO complex was characterized using AFM. AFM analyses revealed the height of P1−GO complex was about 1.7 nm, which was higher than pristine GO (Supporting Information, Figure S1). As expected, the fluorescence of P1 was strongly quenched. Furthermore, the concentration of GO strongly influenced on the fluorescence intensity of P1. With the increasing concentration of GO, the fluorescence intensity of the P1 decreased and trended to a minimum value at 0.5 $\mu$g/mL (Figure 3). Thus, 0.5 $\mu$g/mL GO was used for analytical purposes.

The quenching efficiency [$Q_E$, (%)] of the GO was calculated by using the formula $(1 - \beta) \times 100\%$, where $\beta$ is the ratio of fluorescence of the quenched to the completely dequenched state. The $Q_E$ of GO was calculated to be 94% ± 1.2%. The higher quenching efficiency would lead to a higher signal-to-background ratio and thus better sensitivity and a greater dynamic range for

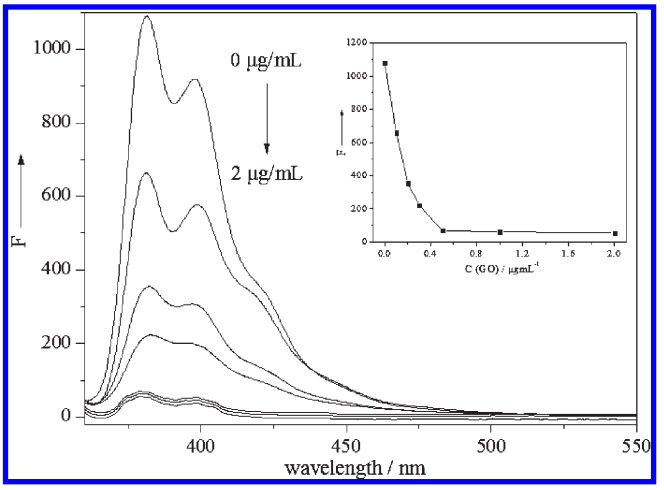


**Figure 3.** Fluorescence quenching of P1 by various concentrations of GO (0, 0.1, 0.2, 0.3, 0.5, 1, 2 $\mu$g/mL). Inset: calibration curve of fluorescence intensity changes at 382 nm as a function of GO concentration.

target detection. In the presence of Ab1, a significant fluorescence enhancement was observed, indicating that the competitive binding of the Ab1 with GO for pyrene-labeled peptide resulted in desorption of pyrene-labeled peptide from the surface of GO (Figure 4A, curve c). Furthermore, the fluorescence intensity of P1 gradually increased as the concentration of Ab1 was increased (Figure 4B). As shown in the inset of Figure 4B, a proportional relationship was observed between the concentration of Ab1 and relative fluorescence intensity of the sensing platform. The assay allowed for the detection of Ab1 at a concentration as low as 200 pM based on three times the signal-to-noise level, which was close to the dissociation constant between peptide and Ab1. The sensitivity of this approach is similar to the nanomolar detection limits reported for most of the best single-step biosensor platforms, such as surface plasmon resonance (SPR),[9] quartz crystal microbalance (QCM),[10] and peptide beacons.[19,20]

**Kinetic Behaviors of the P1−GO Complex with Anti-HIV-1 gp120 Antibody.** The kinetic behaviors of P1 and GO, as well as of the P1−GO complex with Ab1, were studied by monitoring the fluorescence intensity as a function of time. Figure 5 shows the fluorescence quenching of P1 in the presence of GO as a function of incubation time (curve a). The adsorption of P1 on the surface of GO was very fast at room temperature. It reached equilibrium in 1 min. The competitive binding of the Ab1 with GO for pyrene-labeled peptide diminished the GO and P1 contact, resulting in gradual desorption of P1 from the surface of GO. In turn, the fluorescence intensity of P1 gradually increased (curve b). This GO-based approach can monitor kinetics of P1−GO with Ab1 in real time, thus making it more applicable to study peptide−protein interactions.

**Interferences.** The selectivity of the sensing platform described herein has been determined by examining the fluorescence responses of P1−GO complex toward human IgG, human serum albumin (HSA), bovine serum albumin (BSA), hemoglobin, and myoglobin. As shown in Figure 6, the P1−GO complex exhibited little fluorescence response to the nonspecific proteins. This result clearly demonstrated that GO and peptide complex could be used as a sensitive and selective probe for target protein detection.

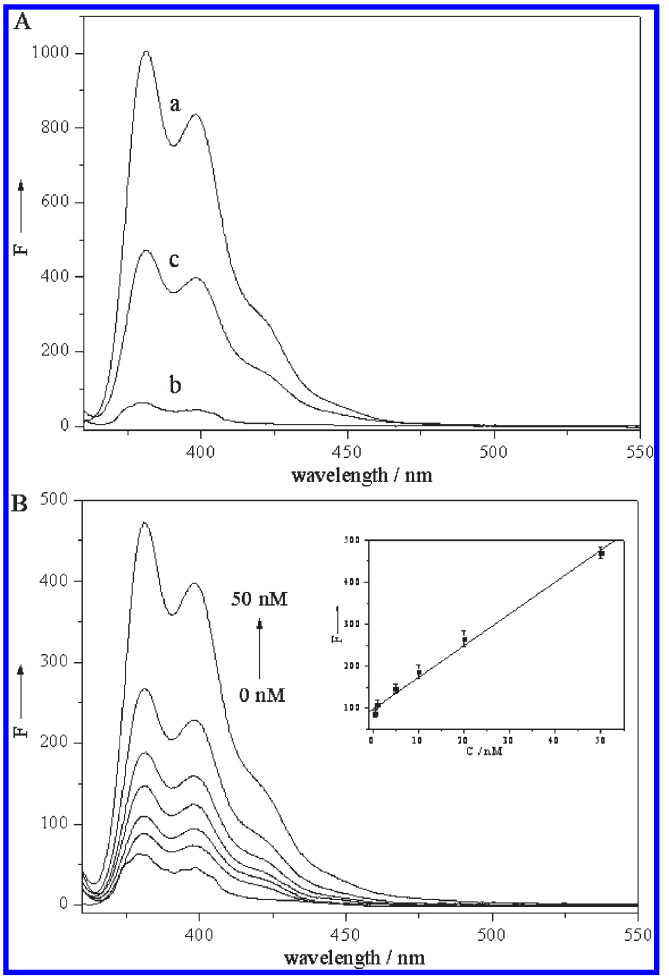


**Figure 4.** (A) Fluorescence emission spectra of (a) P1 (500 nM), (b) P1−GO (0.5 $\mu$g/mL), and (c) P1−GO after incubation with Ab1 (50 nM) for 30 min. Excitation was at 340 nm, and emission was monitored at 382 nm. (B) Fluorescence emission spectra of the assay for Ab1 (0, 0.5, 1, 5, 10, 20, 50 nM). Inset: calibration curve of fluorescence intensity changes at 382 nm as a function of Ab1 concentration. The data shown here represent the means and standard deviations of three independent experiments.

**Detection of the Anti-HIV-1 gp120 Antibody in Complex Samples.** The high selectivity of this approach encourages us further to detect the target protein in complex, contaminant-ridden samples (such as serum and saliva). The analysis of Ab1 in real biological fluids will certainly face the interference of other components, and thus, the determination limits for antibody will need to be further evaluated. Preliminary experiments revealed the detection limit was 2 nM in saliva (Figure 7) and 5 nM in 20% human serum (Figure 8). This proves that our approach is capable of detecting target protein in complex media. Furthermore, pyrene is an environmentally sensitive probe and the excitation occurs in the UV. These result in significant background fluorescence. Further improvements are expected from the choice of environmentally stable fluorescent probes with visible-light excitation such as ruthenium-based fluorescent probes.[20]

**Monitoring the Interactions between Peptide and Anti-HIV-2 gp36 Antibody.** To explore the generalizability of our approach, we applied this approach to detect another anti-HIV antibody, anti-HIV-2 gp36 antibody (Ab2). We chose a specific

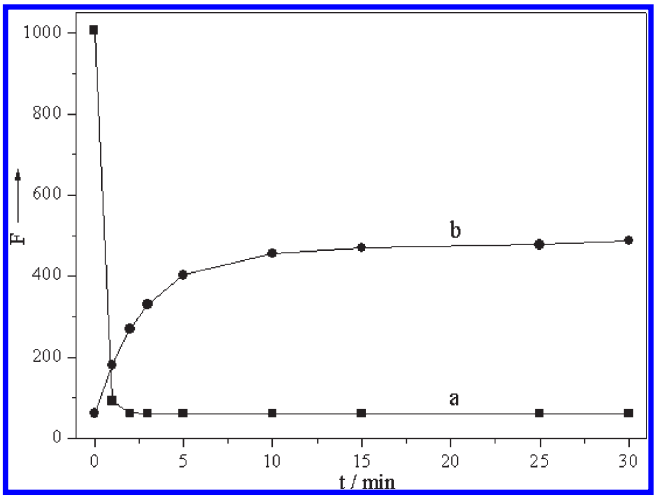


**Figure 5.** (a) Fluorescence quenching of P1 by GO as a function of time and (b) fluorescence restoration of P1−GO by Ab1 (50 nM) as a function of time.

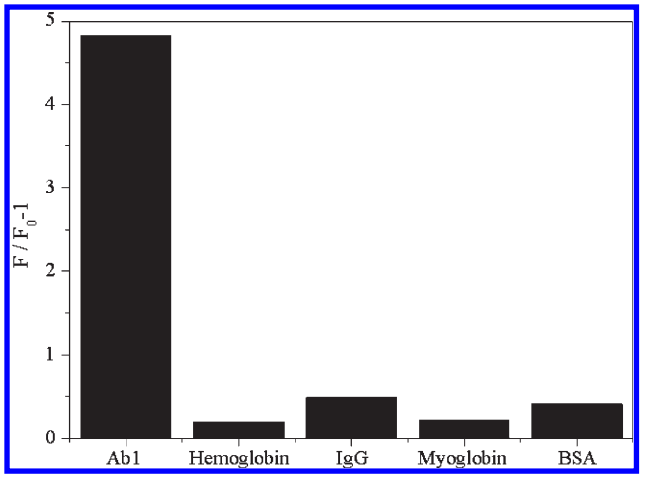


**Figure 6.** Fluorescence intensity changes ($F/F_0 - 1$) of P1 toward Ab1 and different nonspecific proteins. $F_0$ and $F$ are fluorescence intensities at 382 nm in the absence and the presence of antibody, respectively.

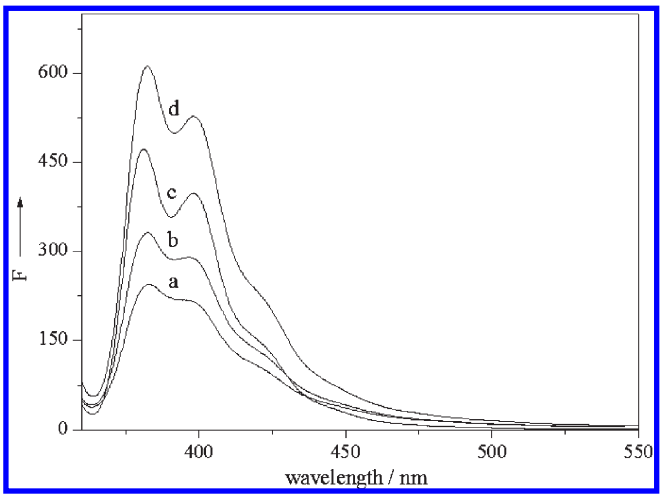


**Figure 7.** Fluorescence emission spectra of P1−GO (0.5 $\mu$g/mL) after incubation with various concentrations of Ab1 (a, 0 nM; b, 2 nM; c, 5 nM and d, 10 nM) in saliva.

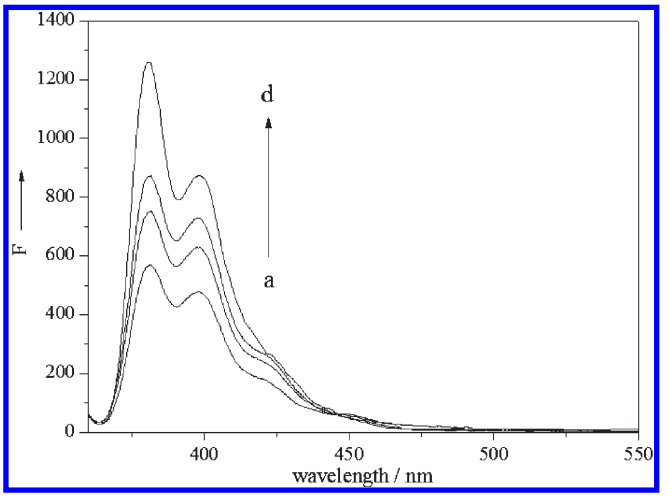


**Figure 8.** Fluorescence emission spectra of P1−GO (0.5 $\mu$g/mL) after incubation with various concentrations of Ab1 (a, 0 nM; b, 5 nM; c, 10 nM; d, 20 nM) in 20% human serum.

immunodominant epitope (11 amino acids) from the transmembrane (gp36) portion of the HIV-2 envelope glycoprotein to synthesis P2 for detection of Ab2.[49,50] As expected, the pyrene derivative of P2 was also strongly quenched by GO. After addition of the Ab2, a dramatic increase in the fluorescence intensity was observed (Figure 9). This result suggested that the proposed approach based on GO and pyrene-labeled peptide complex was general for monitoring peptide−protein interactions.

**Monitoring the Interactions between Peptide and $\alpha$-Bungarotoxin.** To further explore the generalizability of our approach, we have applied our approach to study another peptide−protein interaction (not peptide−antibody). Snake venom $\alpha$-bungarotoxin ($\alpha$-Bgt) is a member of the $\alpha$-neurotoxin family that binds with very high affinity to the nicotinic acetylcholine receptor (AChR) at the neuromuscular junction. A 13-mer peptide (HaPep: WRYYESSLEPYPD) can bind the $\alpha$-Bgt with high affinity, thus inhibiting its interactions with AChR.[51,52] We synthesized a pyrene-labeled peptide (pyrene−HaPep: pyrene−GGGWRYYESSLEPYPD) to study interactions between the $\alpha$-Bgt and peptide. As expected, the fluorescence of the pyrene derivative of the peptide was strongly quenched by GO. After addition of the $\alpha$-Bgt, a dramatic increase in the fluorescence intensity was observed (Supporting Information, Figure S2). This result further suggested that our approach was general for monitoring peptide−protein interactions.

**Fluorescence Anisotropy.** As shown by the experimental data, the proposed approach could work well for probing peptide and protein interactions because of the high sensitivity and selectivity. However, a key question that arises is how the GO and pyrene-labeled peptide complex interact with the target. The fluorescence anisotropy of a fluorophore reflects the ability of the molecule to rotate in its microenvironment, and anisotropy measurements are commonly used to investigate molecular interactions.[53] As shown in Figure 10, the fluorescence anisotropy of P1 in the buffer was 0.083, and it increased 4.43-fold after addition of GO, indicating that the P1 was adsorbed on the GO surface to form P1−GO complex. However, the fluorescence anisotropy decreased by 2.65-fold after further addition of Ab1.

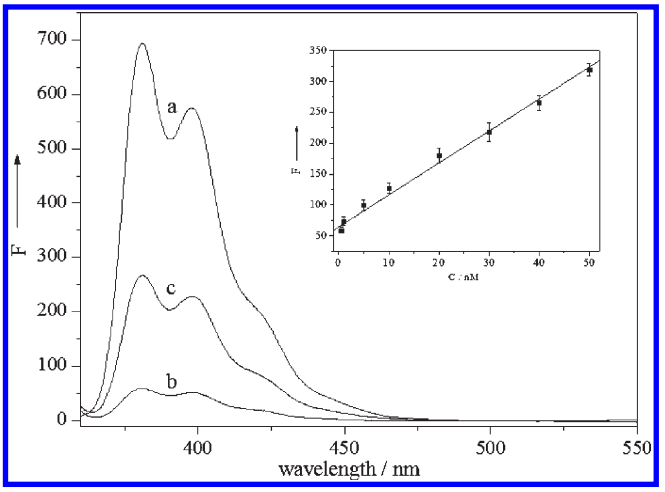


**Figure 9.** Fluorescence emission spectra of (a) P2, (b) P2−GO, and (c) P2−GO after incubation with anti-HIV-2 gp36 antibody (40 nM). Inset: calibration curve of fluorescence intensity changes at 382 nm as a function of anti-HIV-2 gp36 antibody concentration. The data shown here represent the means and standard deviations of three independent experiments. Excitation was at 340 nm.

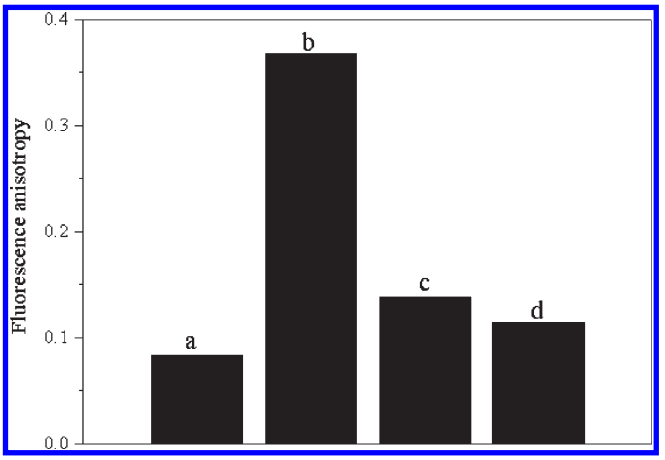


**Figure 10.** Changes of fluorescence anisotropy of (a) P1 (500 nM), (b) P1(500 nM) + GO (0.5 $\mu$g/mL), (c) P1(500 nM) + GO (0.5 $\mu$g/mL) + Ab1 (500 nM), and (d) P1(500 nM) + Ab1 (500 nM).

Furthermore, the value of the fluorescence anisotropy of P1−GO with Ab1 is almost the same as that of free P1 upon addition of A1. These results primarily indicate that the competitive binding of antibody with GO for pyrene-labeled peptide decreased the adsorption of P1 on GO and then P1−antibody complex formed in the solution.

## CONCLUSIONS

In conclusion, we have proposed a simple and general approach for monitoring peptide−protein interactions based on GO and peptide complex. For probing peptide−protein interactions, this platform possesses several excellent features. First, it is simple and cost-effective. This approach requires only one pyrene label, and there is no need for modifying expensive PNA or a fluorophore/quencher pair. The GO, a critical component in the present approach, can be prepared in large quantities from graphite available at very low cost. Second, this approach appears to be more general than previous peptide-based optical approaches. It could be expanded to other targets by changing the sequences of the peptides. Third, the interactions of pyrene-labeled peptides and GO can improve the specificity for the target and substantially suppress background fluorescence. In addition, given the elucidation of large libraries of polypeptide-based recognition elements by phage and bacterial display techniques, it appears that this approach will be applicable to a wide range of macromolecular targets. Taken together, these features suggest that this approach is well-suited for routine laboratory applications. Furthermore, this approach has great potential in drug screening for inhibitors of peptide−protein interactions. This work is underway now in our laboratory and will be communicated in due course.

## ASSOCIATED CONTENT

**Supporting Information.** Additional information as noted in text. This material is available free of charge via the Internet at http://pubs.acs.org.

## AUTHOR INFORMATION

**Corresponding Author**
*E-mail: hhyang@fio.org.cn.

## ACKNOWLEDGMENT

This work was supported by Grants from the National Basic Research Program of China (No. 2010CB732403), the National Natural Science Foundation of China (Nos. 20975023, 20735002), the program for new century excellent talents in university of China (09-0014), and the National Science Foundation of Fujian Province (2010J06003). We thank Danmei Pan from the Fujian Institute of Research on the Structure of Matter, Chinese Academy of Sciences for the AFM characterizations.

## REFERENCES

(1) Cusick, M. E.; Klitgord, N.; Vidal, M.; Hill, D. E. *Hum. Mol. Genet.* **2005**, *14*, R171–R181.
(2) Norman, T. C.; Smith, D. L.; Sorger, P. K.; Drees, B. L.; O'Rourke, S. M.; Hughes, T. R.; Roberts, C. J.; Friend, S. H.; Fields, S.; Murray, A. W. *Science* **1999**, *285*, 591–595.
(3) Ryan, D. P.; Matthews, J. M. *Curr. Opin. Struct. Biol.* **2005**, *15*, 441–446.
(4) Fischer, P. M. *Drug Des. Rev.* **2005**, *2*, 179–207.
(5) Bessette, P. H.; Rice, J. J.; Daugherty, P. S. *Protein Eng., Des. Sel.* **2004**, *17*, 731–739.
(6) Sidhu, S. S. *Curr. Opin. Biotechnol.* **2000**, *11*, 610–616.
(7) Sarikaya, M.; Tamerler, C.; Alex, K. Y. J.; Schulten, K.; Baneyx, F. *Nat. Mater.* **2003**, *2*, 577–585.
(8) Chen, H.; Su, X.; Neoh, K. G.; Choe, W. S. *Langmuir* **2008**, *24*, 6852–6857.
(9) Wegner, G. J.; Wark, A. W.; Lee, H. J.; Codner, E.; Saeki, T.; Fang, S.; Corn, R. M. *Anal. Chem.* **2004**, *76*, 5677–5684.
(10) Cooper, M. A. *Anal. Bioanal. Chem.* **2003**, *377*, 834–842.
(11) Katz, E.; Willner, I. *Electroanalysis* **2003**, *15*, 913–947.
(12) Ziegler, C. *Anal. Bioanal. Chem.* **2004**, *379*, 946–959.
(13) Wei, A. P.; Blumenthal, D. K.; Herron, J. N. *Anal. Chem.* **1994**, *66*, 1500–1506.
(14) Geoghegan, K. F.; Rosner, P. J.; Hoth, L. R. *Bioconjugate Chem.* **2000**, *11*, 71–77.
(15) Neuweiler, H.; Schultz, A.; Vaiana, A. C.; Smith, J. C.; Kaul, S.; Wolfrum, J.; Sauer, M. *Angew. Chem., Int. Ed.* **2002**, *41*, 4769–4773.

(16) Kohn, J. E.; Plaxco, K. W. *Proc. Natl. Acad. Sci. U.S.A.* **2005**, *102*, 10841–10845.
(17) Voss, S.; Fischer, R.; Jung, G.; Wiesmuller, K. H.; Brock, R. *J. Am. Chem. Soc.* **2007**, *129*, 554–561.
(18) Wruss, J.; Pollheimer, P. D.; Meindl, I.; Reichel, A.; Schulze, K.; Schofberger, W.; Piehler, J.; Tampe, R.; Blaas, D.; Gruber, H. J. *J. Am. Chem. Soc.* **2009**, *131*, 5478–5482.
(19) Oh, K. J.; Cash, K. J.; Plaxco, K. W. *J. Am. Chem. Soc.* **2006**, *128*, 14018–14019.
(20) Oh, K. J.; Cash, K. J.; Hugenberg, V.; Plaxco, K. W. *Bioconjugate Chem.* **2007**, *18*, 607–609.
(21) Oh, K. J.; Cash, K. J.; Plaxco, K. W. *Chem.—Eur. J.* **2009**, *15*, 2244–2251.
(22) Thurley, S.; Roglin, L.; Seitz, O. *J. Am. Chem. Soc.* **2007**, *129*, 12693–12695.
(23) Oh, K. J.; Cash, K. J.; Lubin, A. A.; Plaxco, K. W. *Chem. Commun.* **2007**, *43*, 4869–4871.
(24) Novoselov, K. S.; Geim, A. K.; Morozov, S. V.; Jiang, D.; Zhang, Y.; Dubonos, S. V.; Grigorieva, I. V.; Firsov, A. A. *Science* **2004**, *306*, 666–669.
(25) Lomeda, J. R.; Doyle, C. D.; Kosynkin, D. V.; Hwang, W. F.; Tour, J. M. *J. Am. Chem. Soc.* **2008**, *130*, 16201–16206.
(26) Yang, W.; Ratinac, K. R.; Ringer, S. P.; Thordarson, P.; Gooding, J. J.; Braet, F. *Angew. Chem., Int. Ed.* **2010**, *49*, 2114–2138.
(27) Lu, C. H.; Yang, H. H.; Zhu, C. L.; Chen, X.; Chen, G. N. *Angew. Chem., Int. Ed.* **2009**, *48*, 4785–4787.
(28) Lu, C. H.; Zhu, C. L.; Li, J.; Liu, J. J.; Chen, X.; Yang, H. H. *Chem. Commun.* **2010**, *46*, 3116–3118.
(29) Lu, C. H.; Li, J.; Lin, M. H.; Wang, Y. W.; Yang, H. H.; Chen, X.; Chen, G. N. *Angew. Chem., Int. Ed.* **2010**, *49*, 8454–8457.
(30) He, S.; Song, B.; Li, D.; Zhu, C.; Qi, W.; Wen, Y.; Wang, L.; Song, S.; Fang, H.; Fan, C. *Adv. Funct. Mater.* **2010**, *20*, 453–459.
(31) Wang, Y.; Li, Z.; Hu, D.; Lin, C. T.; Li, J.; Lin, Y. *J. Am. Chem. Soc.* **2010**, *132*, 9274–9276.
(32) Dong, H.; Gao, W.; Yan, F.; Ji, H.; Ju, H. *Anal. Chem.* **2010**, *82*, 5511–5517.
(33) Liu, Z.; Robinson, J. T.; Sun, X.; Dai, H. *J. Am. Chem. Soc.* **2008**, *130*, 10876–10877.
(34) Sun, X.; Liu, Z.; Welsher, K.; Robinson, J. T.; Goodwin, A.; Zaric, S.; Dai, H. *Nano Res.* **2008**, *1*, 203–212.
(35) Geim, A. K. *Science* **2009**, *324*, 1530–1534.
(36) Haugland, R. P. *Handbook of Fluorescent Probes and Research Chemicals*, 10th ed.; Molecular Probes: Eugene, OR, 2005.
(37) Yang, C. J.; Jockusch, S.; Vicens, M.; Turro, N. J.; Tan, W. *Proc. Natl. Acad. Sci. U.S.A.* **2005**, *102*, 17278–17283.
(38) Tcherkasskaya, O.; Davidson, E. A.; Schmerr, M. J.; Orser, C. S. *Biotechnol. Lett.* **2005**, *27*, 671–675.
(39) Xu, Y.; Bai, H.; Lu, G.; Li, C.; Shi, G. *J. Am. Chem. Soc.* **2008**, *130*, 5856–5857.
(40) Swathi, R. S.; Sebastian, K. L. *J. Chem. Phys.* **2008**, *129*, 054703–054711.
(41) Balapanuru, J.; Yang, J. X.; Xiao, S.; Bao, Q.; Jahan, M.; Polavarapu, L.; Wei, J.; Xu, Q. H.; Loh, K. P. *Angew. Chem., Int. Ed.* **2010**, *49*, 6549–6553.
(42) Zhang, Y.; Liu, C.; Shi, W.; Wang, Z.; Dai, L.; Zhang, X. *Langmuir* **2007**, *23*, 7911–7915.
(43) Hummers, W. S.; Offeman, R. E. *J. Am. Chem. Soc.* **1958**, *80*, 1339.
(44) Shen, J.; Hu, Y.; Shi, M.; Lu, X.; Qin, C.; Li, C.; Ye, M. *Chem. Mater.* **2009**, *21*, 3514–3520.
(45) Wyatt, R.; Sodroski, J. *Science* **1998**, *280*, 1884–1888.
(46) Freed, E. O.; Martin, M. A. *J. Biol. Chem.* **1995**, *270*, 23883–23886.
(47) Mckeating, J. A.; Shotton, C.; Cordell, J.; Graham, S.; Balfe, P.; Sullivan, N.; Charles, M.; Page, M.; Bolmstedt, A.; Olofsson, S.; Kayman, S. C.; Wu, Z.; Pinter, A.; Dean, C.; Sodroski, J.; Weiss, R. A. *J. Virol.* **1993**, *67*, 4932–4944.
(48) Rajesh, C.; Majumder, C.; Mizuseki, H.; Kawazoe, Y. *J. Chem. Phys.* **2009**, *130*, 124911–124916.
(49) Gnann, J. W.; Mccormick, J. B.; Mitchell, S.; Nelson, J. A.; Oldstone, M. B. *Science* **1987**, *237*, 1346–1349.
(50) Kannangai, R.; Ramalingam, S.; Prakash, K. J.; Abraham, O. C.; George, R.; Castillo, R. C.; Schwartz, D. H.; Jesudason, M. V.; Sridharan, G. *J. Clin. Virol.* **2001**, *22*, 41–46.
(51) Scherf, T.; Kasher, R.; Balass, M.; Fridkin, M.; Fuchs, S.; Katchalski-Katzir, E. *Proc. Natl. Acad. Sci. U.S.A.* **2001**, *98*, 6629–6634.
(52) Spiga, O.; Bernini, A.; Scarselli, M.; Ciutti, A.; Bracci, L.; Lozzi, L.; Lelli, B.; Maro, D. D.; Calamandrei, D.; Niccolai, N. *FEBS Lett.* **2002**, *511*, 33–35.
(53) Lakowicz, J. *Principles of Fluorescence Spectroscopy*, 3rd ed.; Springer: New York, 2006.